Energy Advances

ROYAL SOCIETY OF CHEMISTRY

COMMUNICATION

View Article Online
View Journal | View Issue

Open Access Article. Published on 14 2565. Downloaded on 3/2/2569 20:22:58.
This article is licensed under a Creative Commons Attribution-NonCommercial 3.0 Unported Licence.

Check for updates

Cite this: *Energy Adv.*, 2022, 1, 398

Received 7th June 2022,
Accepted 14th June 2022

DOI: 10.1039/d2ya00135g

rsc.li/energy-advances

An efficient Buchwald–Hartwig amination protocol enables the synthesis of new branched and polymeric hole transport materials for perovskite solar cells†

Erika Ghiglietti,[a] Suresh Podapangi,[b] Sara Mecca,[a] Lorenzo Mezzomo,[a] Riccardo Ruffo,[a] Mauro Sassi,[a] Sara Mattiello,[a] Thomas M. Brown[b] and Luca Beverina*[a]

Perovskite solar cells (PSCs) are experiencing tremendous interest due to compatibility with solution processing on a wide range of substrates and very high efficiency. The hole transport layer (HTL) plays a fundamental role in such multistack cells. We propose new branched and polymeric organic HTL derivatives with sustainable synthesis and performances exceeding those of Spiro-OMeTAD, the standard in the field.

In the last decade, interest in PSCs has grown thanks to their high performance in converting solar energy into electricity.[1,2] Conventional cells are constituted by a conductive substrate (FTO or ITO), an electron transporting material (ETM), a layer of perovskite, a hole transporting layer (HTL), and a metal (Au) electrode.[2–4] The choice of the HTL material is a key point to efficiently collect holes from the perovskite layer, as well as preventing charge recombination.[1,4] New and efficient HTL materials are constantly reported and their properties benchmarked with respect to the reference, commercially available derivative: 2,2′,7,7′-tetrakis[*N*,*N*-di(4-methoxyphenyl)amino]-9,9′-spirobifluorene (Spiro-OMeTAD).[1,2,4] The latter is successful but expensive due to the need for multi-step synthesis and chromatographic purification, both heavily relying on volatile organic solvents (VOCs).[5] The overall impact of Spiro-OMeTAD in PSC technology was recently thoroughly discussed down to the Life Cycle Analysis level, highlighting the strong impact of VOCs.[6] Efforts have been devoted to both improving the synthesis of Spiro-OMeTAD and to the development of alternative materials featuring comparable performances but improved sustainability and reduced cost.[7–9] Mostly, alternative design guidelines focus on the substitution of the 9,9′-spirobifluorene core, due to its multi-step synthetic access, also involving the use of pyrophoric reagents. Alternative viable cores include carbazole, pyrene, phenothiazine, spiro[9*H*-fluorene-9,9′-[9*H*]xanthene], spiro-[cyclopenta[2,1-*b*:3,4-*b*′]dithiophene-4,9′-fluorene], triphenylamine and triazatruxene, to name but a few.[10–14] Very recently, we demonstrated that the synthesis of Spiro-OMeTAD can be dramatically improved by means of a new protocol for the preparation and bromination of 9,9′-spirobifluorene (both safer and cheaper) and thanks to an environmentally respectful Buchwald–Hartwig (B–H) amination protocol, requiring only minimal amounts of VOCs.[15]

In this paper we aim at further exploiting our efficient B–H amination protocol for the synthesis of new branched HTL derivatives featuring a 9,9′-spirobifluorene core, carbazole lateral units, and peripheral electron donating moieties. We also successfully extended the B–H amination to the synthesis of an alternating co-polymer having an aromatic amine and carbazole as the repeating units. The molecular weight and dispersity we obtained are in line with the best results described in the very few already documented B–H polymerizations.[16–19] Good candidate HTL materials should possess a relatively high lying HOMO level (around −5.2 eV), high hole mobility (at least 10^{-3} cm^2 Vs^{-1}), capability to form pinhole free smooth films, high stability, reversible redox behaviour, and poor (or no) tendency toward crystallization. 3-D branched derivatives featuring multiple electron-donating moieties in the periphery fulfil all such requirements.[20] While designing the new derivatives shown in Scheme 1, we kept the 9,9′-spirobifluorene core – which we can now prepare efficiently and in a green chemistry compliant way[15] – and we modified the electron donating periphery by either increasing the number of aromatic amines *via* the introduction of a further carbazole branching point (derivatives **6** and **7**) or by substituting the established bis(4-methoxyphenyl)amine donor with 5*H*-dibenzo[b,f]azepine (derivative **8**) whose central 7-membered ring is formally antiaromatic and should consequently behave as a particularly good donor.[21,22]

[a] *Department of Materials Science, University of Milano-Bicocca and INSTM, Via R. Cozzi, 55, I-20125 Milan, Italy. E-mail: luca.beverina@unimib.it*

[b] *CHOSE (Centre for Hybrid and Organic Solar Energy), Department of Electronic Engineering, University of Rome Tor Vergata, Via del Politecnico 1, I-00133 Rome, Italy*

† Electronic supplementary information (ESI) available: Synthetic details; thermal and electrochemical characterization of the materials used as a HTL; details on PSC fabrication and performances; NMR spectra of known and original derivatives. Complete ref. 29 and 31. See DOI: https://doi.org/10.1039/d2ya00135g

© 2022 The Author(s). Published by the Royal Society of Chemistry

Open Access Article. Published on 14 2565. Downloaded on 3/2/2569 20:22:58.
This article is licensed under a Creative Commons Attribution-NonCommercial 3.0 Unported Licence.

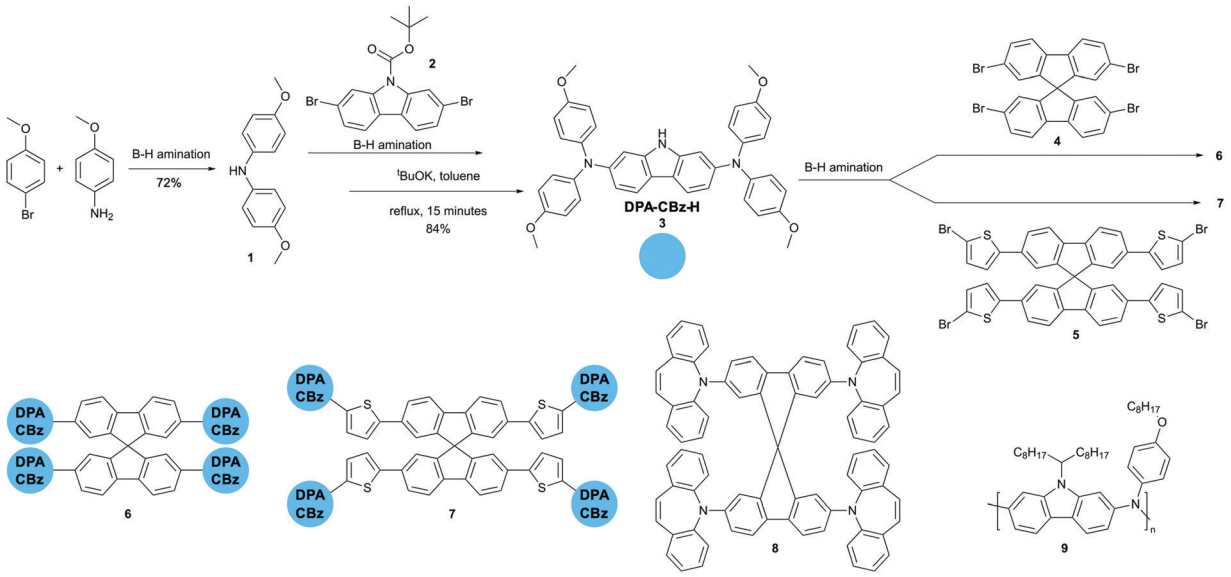

Scheme 1 Synthesis by B–H amination of bis(4-methoxyphenyl)amine, N^2,N^2,N^7,N^7-tetrakis(4-methoxyphenyl)-9*H*-carbazole-2,7-diamine (**DPA-CBz-H**), and derivatives **6** and **7**. Structures of derivatives **8** (obtained by B–H coupling between **4** and 5*H*-dibenzo[*b*,*f*]azepine) and **9** (obtained by B–H coupling between 2,7-dibromo-9-(1-octylnonyl)-9*H*-carbazole and 4-octyloxyphenylamine).

The synthesis of the molecular derivatives is a convergent approach requiring sequential B–H aminations. B–H can be carried out both under micellar catalysis in aqueous solutions of surfactants, and in solventless conditions.[23–26] We very recently demonstrated that both protocols are efficient in the final step of Spiro-OMeTAD synthesis.[15] We obtained the best results using $Pd(OAc)_2$/XPhos as the catalyst, K_3PO_4 as the base, PEG 2000 dimethylether as the phase transfer catalyst and 25 wt% of toluene with respect to the whole reaction mass as a mixing aid. Scheme 1 shows that working under the very same conditions, we prepared 4,4′-dimethoxydiphenylamine (**1**) in 72% yield from inexpensive starting compounds. The same can be coupled under identical conditions with *N*-Boc-2,7-dibromocarbazole, yielding derivative **3** in 84% overall yield, after deprotection of the carbazole nitrogen in refluxing toluene and in the presence of ^{t}BuOK. A further B–H amination leads to derivative **6** in 25% yield, when reacting **3** with 2,2′,7,7′-tetrabromo-9,9′-spirobifluorene **4**. Under identical conditions we prepared derivative **7** in 34% yield, by coupling **3** with 2,2′,7,7′-tetrakis(5-bromothiophen-2-yl)-9,9′-spirobifluorene **5**. The synthesis of the original derivative **5** requires Suzuki–Miyaura coupling under micellar catalysis conditions of **4** with 5 equivalents of thiophene-2-boronic acid, followed by bromination (see ESI†). Finally, we prepared **8** by reaction of **4** with excess 5*H*-dibenzo[*b*,*f*]azepine – a substrate we already employed in B–H reactions in the past[27,28] – in 40% yield.

Having assessed the robustness of the reaction conditions, we challenged them in a polymerization reaction. The literature reports very few examples of B–H polymerizations,[16–19] only in one case leading to a polymer (an aromatic amine-dialkylfluorene alternating copolymer) having applications in electronic devices.[16] We selected 2,7-dibromo-9-(1-octylnonyl)-9*H*-carbazole and 4-octyloxyaniline as the co-monomers according to both the similarity of the structure to the previously reported B–H polymer and to the superior performances as semiconductors in both OFETs and OPVs of polymers incorporating carbazole in the place of fluorene. Without any optimization of the reaction conditions, we obtained polymer **9** with M_n = 20 400 and $Đ$ = 1.72 in a very remarkable 76% yield, after refinement of the molecular weights by sequential Soxhlet extraction. Such values are in line with the best ones previously reported.[16–18] We submitted all new materials to a complete electrochemical (Cyclic Voltammetry), thermal (DSC-TGA) and stability (NMR) characterization and we compared the results with Spiro-OMeTAD tested under identical conditions (see ESI,† Fig. S18–S36). All new derivatives feature reversible redox behaviour, with comparable potentials for the first oxidation process. The dibenzoazepine substituted derivative **8** (HOMO = −4.91 eV) and polymer **9** (HOMO = −4.93 eV) feature HOMO levels aligned with that of Spiro-OMeTAD (HOMO = −4.95 eV under our conditions). Derivatives **6** (HOMO = −4.78 eV) and **7** (HOMO = −4.80 eV) have very similar energy levels, slightly more positive than that of Spiro-OMeTAD. The DSC-TGA analysis (see ESI†) of derivative **6** shows no clearly distinguishable melting point at the first heating cycle, nor a crystallization peak while cycling. In contrast, Spiro-OMeTAD and **8** DSC traces show a thermally induced crystallization during the first heating cycle, followed by melting. In the case of derivative **7**, we again observed the thermally induced crystallization during the first heating cycle, but no melting (Fig. 1A).

We compared the ^{1}H-NMR spectrum of all materials prior to and after the thermal analysis to assess the stability up to 250 °C, evidencing the formation of minor decomposition products only in the case of Spiro-OMeTAD. Fig. 1B shows the aromatic portion of the spectra collected for derivative **7** (see ESI† for other derivatives). UV-Vis absorption profiles of materials

Open Access Article. Published on 14 2565. Downloaded on 3/2/2569 20:22:58.
This article is licensed under a Creative Commons Attribution-NonCommercial 3.0 Unported Licence.

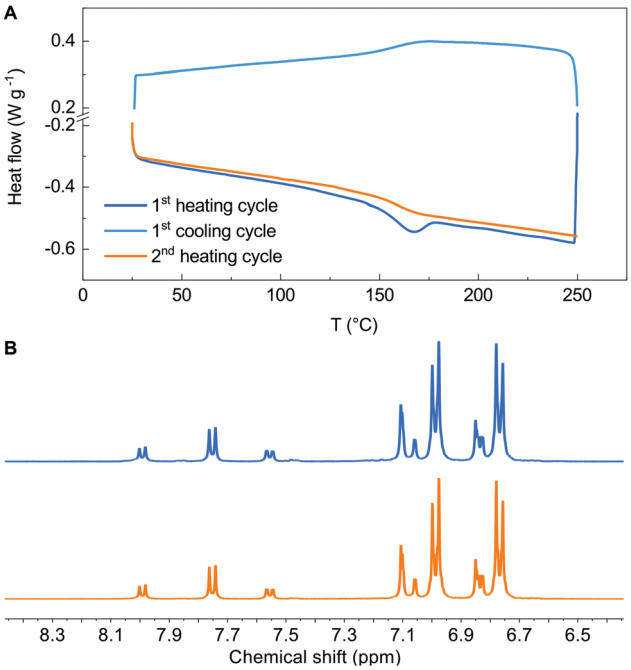

Fig. 1 (A) DSC characterization of derivative **7**. (B) Details of the aromatic portion of the ^{1}H NMR spectra in THF-d_8 of derivative **7** before (blue line) and after (orange line) the DSC thermal treatment.

6–9 aren't significantly different from those of Spiro-OMeTAD, thus enabling direct comparison (see ESI†). We thus tested the performances of all materials as a HTL in PSCs.

We fabricated cells on glass substrates having the architecture glass/ITO/SnO_2/$Cs_{0.06}FA_{0.78}MA_{0.16}Pb(I_{0.84}Br_{0.16})_3$(FAMACs)/HTM/Au, optimized for previous comparative studies. Fig. 2 shows the *J–V* graphs for the best solar cells that we obtained, where the HTM is either the reference commercial Spiro-OMeTAD (purchased by Borun New Material Technology LTD) or the newly synthesized materials, measured both from the reverse (RV) current–voltage scan (from V_{OC} to $V = 0$) and the forward (FW) current–voltage scan (from $V = 0$ to V_{OC}). The power conversion efficiency (PCE) of the triple cation perovskite solar cells is very much dependent on the details of the deposition procedure and the composition of the different layers in the stack. PV cells based on the very same PVK phase can give PCEs in the 12–20% range according to a recent literature survey.[29]

The average PCE value of 14.6% that we obtained for cells prepared with commercial Spiro-OMeTAD corresponds to the vast majority of reported PCEs for this class of PCSs. We thus assume our reference value to be meaningful for the comparative ranking of the HTL performances of the newly synthesized materials. We compared the characteristics of cells prepared with the new HTL in terms of percentage with respect to the values we obtained for the reference Spiro-OMeTAD cell (Fig. 3). All new derivatives feature very high FF values, exceeding that of the reference for both **6** and **7** and equalling it for **9**. As for the V_{OC}, only derivative **7** matches the reference. There is no direct connection between this trend and that of the electrochemical HOMO levels; as such, the different behaviour of the various HTLs is likely to be ascribed to defects at the interphases between the HTL and PVK layers.[30] The J_{sc} values are in all cases smaller than those measured for the control cell, yet overall the PCE that we measured for derivative **7** (15.4 ± 0.8%) exceeds that of the reference cell (14.6 ± 1.6%) by 5.5%. Derivative **6** gave a PCE corresponding to 95.1% of the value of the standard, while the derivative **9** performances were limited to 84% of the standard (Fig. 3). We also measured the external quantum efficiency (EQE) of the cells to analyse the different spectral conversion efficiency for the three different HTMs. As shown in Fig. S39 (ESI†), the EQE spectra have a similar shape for the three materials. EQEs above 80% were observed for Spiro-OMeTAD, **6** and **7** based devices, while the use of **9** HTM gave a lower EQE. The integrated J_{SC} calculated from the EQE spectrum is coherent within the experimental error with the photocurrents. An important factor affecting the development of perovskite solar cells is their stability. Stability experiments were carried out according to the ISOS-D-1 shelf life protocol in which devices were stored in the dark (RH < 40%) at room temperature and tested over time.[31] Within the statistical errors, the cells with all derivatives are at least as good as those made with their commercial Spiro-OMeTAD reference. Derivative **9** is slightly more stable than all branched ones, including Spiro-OMeTAD, thus offering the best overall efficiency/stability trade off in the series (see ESI† for details).

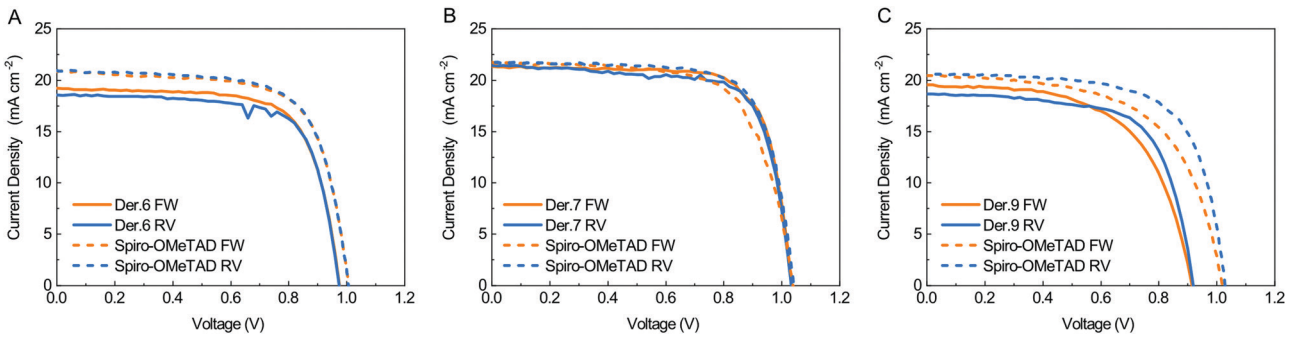

Fig. 2 *J–V* graphs for the best PSCs obtained using derivatives **6** (graph A), **7** (graph B) and **9** (graph C) as the HTL. In each graph, both the forward (orange) and reverse (blue) scan are shown, for both the chosen derivative (full line) and a reference PSC (dashed line) produced using Spiro-OMeTAD as the HTL.

 © 2022 The Author(s). Published by the Royal Society of Chemistry

Open Access Article. Published on 14 2565. Downloaded on 3/2/2569 20:22:58.
This article is licensed under a Creative Commons Attribution-NonCommercial 3.0 Unported Licence.

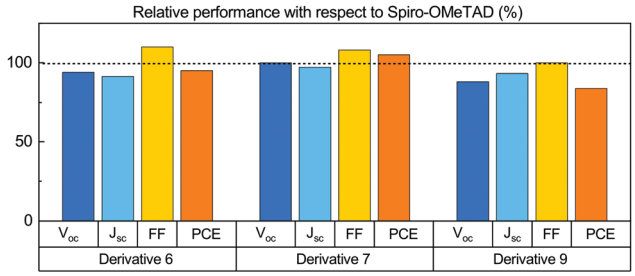

Fig. 3 Average V_{OC}, J_{sc}, FF and PCE of PSCs prepared with derivatives **6**, **7** and **9**, with respect to the average values obtained for reference devices prepared using Spiro-OMeTAD as the HTL.

In conclusion, we have designed and synthesized in a green chemistry compliant way two new HTL materials featuring a 9,9′-spirobifluorene core and carbazole branching units. HTL 7 slightly outperforms the PCE obtained with Spiro-OMeTAD under identical conditions. The key synthetic step to our approach is a very efficient B–H amination requiring minimal amounts of organic solvents. We extended this protocol to the straightforward synthesis of one of the very few examples of B–H polymer showing performances over 84% with respect to those measured with Spiro-OMeTAD, but significantly better stability. Our B–H amination protocol and the new HTL materials that we prepared will contribute to improving the sustainability of the PSC technology.

Conflicts of interest

There are no conflicts to declare.

Acknowledgements

This work was supported by MIUR under a 2017YXX8AZ PRIN grant.

Notes and references

1 H. D. Pham, T. C. Yang, S. M. Jain, G. J. Wilson and P. Sonar, *Adv. Energy Mater.*, 2020, **10**, 1903326.
2 M. Zhang, D. Zhao, L. Chen, N. Pan, C. Huang, H. Cao and M. Chen, *Sol. Energy Mater. Sol. Cells*, 2018, **176**, 318–323.
3 D. Li, J. Shao, Y. Li, Y. Li, L. Deng, Y. Zhong and Q. Meng, *Chem. Commun.*, 2018, **54**, 1651–1654.
4 X. Zhao and M. Wang, *Mater. Today Energy*, 2018, **7**, 208–220.
5 P. Roy, N. Kumar Sinha, S. Tiwari and A. Khare, *Sol. Energy*, 2020, **198**, 665–688.
6 N. Espinosa, L. Serrano-Luján, A. Urbina and F. C. Krebs, *Sol. Energy Mater. Sol. Cells*, 2015, **137**, 303–310.
7 M. Daskeviciene, S. Paek, Z. Wang, T. Malinauskas, G. Jokubauskaite, K. Rakstys, K. T. Cho, A. Magomedov, V. Jankauskas, S. Ahmad, H. J. Snaith, V. Getautis and M. K. Nazeeruddin, *Nano Energy*, 2017, **32**, 551–557.
8 M. L. Petrus, T. Bein, T. J. Dingemans and P. Docampo, *J. Mater. Chem. A*, 2015, **3**, 12159–12162.
9 B. Xu, D. Bi, Y. Hua, P. Liu, M. Cheng, M. Grätzel, L. Kloo, A. Hagfeldt and L. Sun, *Energy Environ. Sci.*, 2016, **9**, 873–877.
10 I. García-benito, I. Zimmermann, J. Urieta-mora, J. Aragó, J. Calbo, J. Perles, A. Serrano, A. Molina-ontoria and E. Ortí, *Adv. Funct. Mater.*, 2018, **28**, 1801734.
11 F. Zhang, S. Wang, H. Zhu, X. Liu, H. Liu, X. Li, Y. Xiao, S. M. Zakeeruddin and M. Grätzel, *ACS Energy Lett.*, 2018, **3**, 1145–1152.
12 W. Huang and S. L. Buchwald, *Chem. – Eur. J.*, 2016, **22**, 14186–14189.
13 X. Chen, A. Ichige, J. Chen, I. Fukushima, J. Kuwabara and T. Kanbara, *Polymer*, 2020, **207**, 122927.
14 P. Gratia, A. Magomedov, T. Malinauskas, M. Daskeviciene, A. Abate, S. Ahmad, M. Grätzel, V. Getautis and M. K. Nazeeruddin, *Angew. Chem., Int. Ed.*, 2015, **54**, 11409–11413.
15 S. Mattiello, G. Lucarelli, A. M. Calascibetta, L. Polastri, E. Ghiglietti, S. Kumar Podapangi, T. M. Brown, M. Sassi and L. Beverina, *ACS Sustainable Chem. Eng.*, 2022, **14**, 4750–4757.
16 R. S. Sprick, M. Hoyos, M.-T. Chen, M. L. Turner and O. Navarro, *J. Polym. Sci., Part A: Polym. Chem.*, 2013, **51**, 4904–4911.
17 M. Hoyos, R. S. Sprick, C. Wang, M. L. Turner and O. Navarro, *J. Polym. Sci., Part A: Polym. Chem.*, 2012, **50**, 4155–4160.
18 R. Grisorio and G. P. Suranna, *Polym. Chem.*, 2019, **10**, 1947–1955.
19 X. Chen, A. Ichige, J. Chen, I. Fukushima, J. Kuwabara and T. Kanbara, *Polymer*, 2020, **207**, 122927.
20 G.-W. Kim, H. Choi, M. Kim, J. Lee, S. Y. Son and T. Park, *Adv. Energy Mater.*, 2020, **10**, 1903403.
21 L. J. Kricka and A. Ledwith, *Chem. Rev.*, 1974, **74**, 101–123.
22 A. Sanguineti, M. Sassi, R. Turrisi, R. Ruffo, G. Vaccaro, F. Meinardi and L. Beverina, *Chem. Commun.*, 2013, **49**, 1618–1620.
23 E. B. Landstrom, N. Akporji, N. R. Lee, C. M. Gabriel, F. C. Braga and B. H. Lipshutz, *Org. Lett.*, 2020, **22**, 6543–6546.
24 T. N. Ansari, A. Taussat, A. H. Clark, M. Nachtegaal, S. Plummer, F. Gallou and S. Handa, *ACS Catal.*, 2019, **9**, 10389–10397.
25 B. H. Lipshutz, D. W. Chung and B. Rich, *Adv. Synth. Catal.*, 2009, **351**, 1717–1721.
26 Y. Zhang, B. S. Takale, F. Gallou, J. Reilly and B. H. Lipshutz, *Chem. Sci.*, 2019, **10**, 10556–10561.
27 G. Vaccaro, A. Bianchi, M. Mauri, S. Bonetti, F. Meinardi, A. Sanguineti, R. Simonutti, L. Beverina and M. Mauri, *Chem. Commun.*, 2013, **49**, 8474–8476.
28 A. Sanguineti, M. Sassi, R. Turrisi, R. Ruffo, G. Vaccaro, F. Meinardi and L. Beverina, *Chem. Commun.*, 2013, **49**, 1618–1620.
29 T. J. Jacobsson, A. Hultqvist, A. Garcqvist, K. A. Anand, A. Al-Ashouri, A. Hagfeldt, A. Crovetto, A. Abate, A. G. Ricciardulli and A. Vijayan, *et al.*, *Nat. Energy*, 2022, **7**, 107–115.
30 N. Wu, Y. Wu, D. Walter, H. Shen, T. Duong, D. Grant, C. Barugkin, X. Fu, J. Peng, T. White, K. Catchpole and K. Weber, *Energy Technol.*, 2017, **5**, 1827–1835.
31 M. O. Reese, S. A. Gevorgyan, M. J.vorgyan, E. Bundgaard, S. R. Kurtz, D. S. Ginley, D. C. Olson, M. T. Lloyd, P. Morvillo and E. A. Katz, *et al.*, *Sol. Energy Mater. Sol. Cells*, 2011, **95**, 1253–1267.